SPANDIDOS PUBLICATIONS

INTERNATIONAL JOURNAL OF ONCOLOGY 63: 87, 2023

Histone lysine demethylase 3B regulates autophagy via transcriptional regulation of *GABARAPL1* in acute myeloid leukemia cells

YING SONG[1], JIAQI ZHANG[1,2], HAIHUA WANG[1,2], HAIYING WANG[1], YONG LIU[1] and ZHENBO HU[1]

[1]Department of Hematology, Laboratory for Stem Cell and Regenerative Medicine, Affiliated Hospital of Weifang Medical University, Weifang, Shandong 261042; [2]Granduate School, Weifang Medical University, Weifang, Shandong 261053, P.R. China

Received April 4, 2023; Accepted June 1, 2023

DOI: 10.3892/ijo.2023.5535

Abstract. Macroautophagy (hereafter referred to as autophagy) is a highly conserved self-digestion process that is critical for maintaining homeostasis in response to various stresses. The autophagy-related protein family, including the GABA type A receptor-associated protein (GABARAP) and microtubule-associated protein 1 light chain 3 subfamilies, is crucial for autophagosome biogenesis. Although the regulatory machinery of autophagy in the cytoplasm has been widely studied, its transcriptional and epigenetic regulatory mechanisms still require more targeted investigations. The present study identified histone lysine demethylase 3B (KDM3B) as a crucial component of autophagy on a panel of leukemia cell lines, including K562, THP1 and U937, resulting in transcriptional activation of the autophagy-related gene *GABA type A receptor-associated protein like 1 (GABARAPL1)*. KDM3B expression promoted autophagosome formation and affected the autophagic flux in leukemia cells under the induction of external stimuli. Notably, RNA-sequencing and reverse transcription-quantitative PCR analysis showed that *KDM3B* knockout inhibited the expression of *GABARAPL1*. Chromatin immunoprecipitation-quantitative PCR and luciferase assay showed that KDM3B was associated with the *GABARAPL1* gene promoter under stimulation and enhanced its transcription. The present findings demonstrated that KDM3B was critical for regulating the *GABARAPL1* gene and influencing the process of autophagy in leukemia cells. These results provide a new insight for exploring the association between autophagy and KDM3B epigenetic regulation in leukemia.

Correspondence to: Professor Zhenbo Hu, Department of Hematology, Laboratory for Stem Cell and Regenerative Medicine, Affiliated Hospital of Weifang Medical University, 4948 Shengli Street East, Weifang, Shandong 261042, P.R. China
E-mail: huzhenbo@wfmc.edu.cn

Key words: histone lysine demethylase 3B, transcriptional regulation, GABA type A receptor-associated protein like 1, autophagy, leukemia

Introduction

Autophagy is an evolutionarily catabolic process that is activated when cells encounter stress, such as nutrient starvation, energy-limiting conditions, endoplasmic reticulum stress and reactive oxygen species. It involves the degradation of unessential proteins or other components. Dysregulation of autophagy contributes to multiple diseases, including cancer and neurodegenerative diseases. In addition, autophagy is essential for maintaining cellular homeostasis in eukaryotes through a mechanism that can be described as a lysosome-dependent degradation of intracellular components.

Under normal conditions, basal autophagy is critical in regulating cell proliferation, apoptosis, differentiation, development, hematopoiesis, inflammation and aging. Dysfunctional autophagy is associated with various diseases, including cancer, diabetes, myopathies, cell death, aging, and neurodegenerative, cardiovascular, heart, lung, infectious and autoimmune diseases (1-6). Mosaic deletion of Atg5 or liver-specific deletion of Atg7 resulted in benign liver adenoma and accumulation of sequestosome 1 (SQSTM1)/p62 in hepatocytes (7). Loss of function for ATG5 has also been found in patients with gastrointestinal cancer, and these ATG5 dysfunctions may interfere with normal apoptosis and autophagy during gastrointestinal cancer pathogenesis (8). Mutations of specific tumor suppressor genes such as ultraviolet irradiation resistance-associated gene (UVRAG) and Beclin 1 (BECN1) could also lead to reduced clearance of intracellular damage components, thereby causing tumor development (9). In addition, the loss of UVRAG or BECN1 was associated with gastric, colon, breast and prostate cancer, as well as hepatocellular and cervical squamous cell carcinoma (10).

Leukemia is a hematological malignancy caused by abnormal proliferation and differentiation of hematopoietic stem cells. It is a clonal hematological tumor characterized by the proliferation and accumulation of lymphoid or myeloid progenitor cells in the entire bone marrow and the blocking of their differentiation. Drug resistance remains an important cause of treatment

failure and high mortality in leukemia. Previous studies focused on autophagy regulation and leukemia treatment demonstrated the ability for autophagy to degrade fusion oncoproteins, including promyelocytic leukemia-retinoic acid receptor α and breakpoint cluster region-Abelson kinase, and then promote leukemic cell death (11-14). Conditional deletion of Atg7 in hematopoietic stem cells (HSCs) affected autophagy activity and led to invasive myeloproliferation and death in mice (15). Low autophagy levels and high NOTCH signaling levels in HSCs were evident in patients with acute myeloid leukemia (AML). Low autophagy also upregulated the NOTCH signaling pathway in mouse models (16). Akt-mTOR, a critical regulatory pathway in autophagy, was also vital for the maintenance of HSCs. It could maintain the balance between self-renewal and differentiation of HSCs, and prevented the transformation of HSCs into leukemia stem cells (17). Unc51-like autophagy activating kinase 1 (ULK1) is a substrate of caspase-3, and ULK1-induced autophagy suppressed leukemogenesis caused by the fusion oncoprotein acute myeloid gene 1 (AML1)-myeloid transforming gene 8 (ETO) in AML (18).

Although autophagy is a cytoplasmic event and the majority of studies have focused on protein-level signaling in the cytoplasm, transcriptional and epigenetic regulation of various autophagy components in the nucleus is also critical. In addition, various histone modifications provide essential functions in the autophagy process. As an increasing number of transcription factors become widely studied in autophagy, including transcription factor EB (TFEB) (19, 20), E2F transcription factor 1 (21,22), and forkhead box proteins of class O subgroup family members (23-26), the associated epigenetic mechanisms involved in controlling chromatin recognition of transcription factors are also receiving more research attention (27). The deubiquitinase ubiquitin specific peptidase 44 affected autophagy by downregulating H2B monoubiquitination under starvation conditions (28). G9a, a methyltransferase, directly suppressed the transcriptional activation of key regulators of autophagy genes by remodeling the chromatin landscape (29). In addition, G9a depletion in *Drosophila melanogaster* suppressed autophagy by altering the expression level of Atg8a in a methyltransferase-independent manner (30). The methyltransferase enhancer of zeste homolog 2 inhibited autophagy via activation of the mTOR signaling pathway, which revealed a new link between autophagy, epigenetic regulation and tumorigenesis in human colorectal carcinoma (31). The histone acetyltransferase hMOF (also called KAT8 or MYST1) and NAD^+-dependent deacetylase sirtuin 1 regulate the H4K16 acetylation levels of autophagy-related genes, which determine cell survival (32). Arginine methyltransferase 1 functions as a co-activator of TFEB and regulates histone H3R17 methylation levels of autophagy-related and lysosomal genes after nutrient starvation (20).

Cytogenetic deletions involving the long arm of chromosome 5 are frequently observed in malignant bone marrow diseases, including myelodysplasia and AML. The affected patients exhibit drug resistance, rapid disease progression and short survival. KDM3B is one of the genes prone to be lost on chromosome 5 (33). As a histone demethylase, KDM3B has a Jumonji C domain, which is mutated or deleted in numerous diseases and tumors, such as breast cancer (34) and myeloid leukemia (35). KDM3s (including KDM3A, KDM3B and Jumonji Domain Containing 1C) regulate chromatin stability and transcription in human colorectal cancer stem cells through synergistic Wnt/β-catenin signaling, thus controlling their tumorigenic potential (36). A previous study showed that KDM3B played a key role in regulating the cell cycle and proliferation of HepG2 cells (37). In addition, KDM3B plays critical roles in prostate cancer genesis (38), ferroptosis (39), differentiation of functional spermatogonia in mice (40) and maintenance of genomic stability (41). Moreover, KDM3B has been investigated in previous studies on hematopoiesis and leukemia, since it acts as a tumor suppressor gene in AML (42,43) and can regulate the expression of the leukemia oncogene LIM domain only 2 (44). H4R3me2s and H3K9me2 could be demethylated by KDM3B to promote gene expression in the development of hematopoietic stem and progenitor cells (45). Despite the currently available knowledge about KDM3B in other aspects, the molecular mechanisms underlying the role of KDM3B in regulating autophagy in leukemia remain unclear.

The present study identified the molecular basis by which KDM3B regulates the transcription of the autophagy-related gene *GABARAPL1* in the leukemia cell lines K562, THP1 and U937. In addition, it was found that the expression of KDM3B promoted the formation of autophagosomes in leukemia cells under stimulations. The present findings reveal the mechanism that KDM3B employs to regulate autophagy as an epigenetic regulator within leukemia cells.

Materials and methods

Antibodies and reagents. The following antibodies were used in the present study: Anti-light chain 3 β (LC3B) [Sigma-Aldrich; Merck KGaA; cat. no. L7543; 1:1,000 for western blotting (WB) and 1:500 for immunofluorescence (IF)], anti-SQSTM1 (Abcam; cat. no. ab109012; 1:5,000 for WB), anti-GABARAPL1 (Cell Signaling Technology, Inc.; cat. no. 26632T; 1:1,000 for WB), anti-H3K9me2 (ABclonal Biotech Co., Ltd.; cat. no. A2359; 1:1,000 for WB), anti-H4R3me2s (ABclonal Biotech Co., Ltd.; cat. no. A3159; 1:1,000 for WB), anti-KDM3B [Invitrogen; Thermo Fisher Scientific, Inc.; cat. no. PA5-17170; 1:1,000 for WB; and Cell Signaling Technology, Inc.; cat. no. 5377S; 1:200 for chromatin immunoprecipitation (ChIP)], anti-GAPDH (Proteintech Group, Inc.; cat. no. 60004-1-Ig; 1:20,000 for WB), horseradish peroxidase (HRP)-labeled secondary antibody conjugates (ABclonal Biotech Co., Ltd.; cat. nos. AS003 and AS014) and Cy3-labeled goat anti-rabbit IgG (H + L) (Beyotime Institute of Biotechnology; cat. no. A0516; 1:300 for IF).

DAPI was purchased from Beijing Solarbio Science & Technology Co., Ltd. (cat. no. S2110), while bafilomycin A1 (BafA1) was obtained from Sigma-Aldrich; Merck KGaA (cat. no. 196000; 100 nM; 2 h for autophagy flux), rapamycin from MedChemExpress (cat. no. HY-10219; 5 μM for autophagy induction) and puromycin from Beijing Solarbio Science & Technology Co., Ltd. (cat. no. P8230; 2 μg/ml for cell screening).

Plasmid constructs. The full-length human *KDM3B* (NM_016604) was cloned into the GV367 vector (Shanghai GeneChem Co., Ltd.), and a plasmid encoding Flag-tagged wild-type (WT) *KDM3B* was constructed.

Cell culture, transfection and generation of knockout (KO) cells. The human cell lines used in the present study were obtained from the Leibniz-Institute DSMZ-German Collection of Microorganisms and Cell Cultures. The cell types of the three cell lines are as follow: K562 (chronic myeloid leukemia in blast crisis), THP1 (acute monocytic leukemia) and U937 (acute monocytic leukemia). All the three cell lines used in the present study have been authenticated using the standard STR (short tandem repeats) genotyping method. The three cell lines were cultured in RPMI-1640 medium (Cellmax Technologies; cat. no. CGM112.05), while 293T cells (Leibniz-Institute DSMZ-German Collection of Microorganisms and Cell Cultures; cat. no. ACC 635) were cultured in DMEM (Cellmax Technologies; cat. no. CGM101.05). The aforementioned media contained 10% fetal bovine serum (FBS) (Cellmax Technologies; cat. no. SA211.02). Cells were incubated in a 5% CO_2-humidified incubator at 37˚C.

For transfection, 293T cells were cultured in cell plates using Lipofectamine® 3000 (Invitrogen; Thermo Fisher Scientific, Inc.; cat. no. L3000015). For starvation treatments, the cells were cultured in Earle's Balanced Salt Solution (EBSS) (Beijing Solarbio Science & Technology Co., Ltd.; cat. no. H2020) for various durations.

To generate *KDM3B* KO cells, lentiviral supernatant containing targeting sequence to *KDM3B* (purchased from Shanghai GeneChem Co., Ltd.) was transfected into target cells (K562, THP1, U937 and 293T). Briefly, *KDM3B* KO cell lines were constructed using the CRISPR/CAS9 lentivirus packaging technique. The targeting gRNA sequence was constructed into lentivirus vector Lenti-sgRNA-CAS9 (cat. no. GV392; Shanghai GeneChem Co., Ltd.), and the lentiviral supernatant was added to the cells in medium containing 10% FBS, centrifuged at 1,000 x g for 1 h at room temperature, and then incubated in a 5% CO_2-humidified incubator at 37˚C. After 2 days of viral infection, 2 μg/ml puromycin was added to the cell culture medium to screen positive cells. After 2 weeks of screening, multiple monoclonal cell colonies were selected using a 96-well plate by the limited dilution method. Multiple cell lines with different KO levels were obtained by monoclonal amplification culture. When the cells proliferated to >$1x10^6$ cells, the cells were collected for WB with an anti-KDM3B antibody. A monoclonal cell colony with complete *KDM3B* KO was selected for each cell line for subsequent experiments. The targeting sequence was as follows: 5'-GTCCAATGGTGTTCTAGCCA-3'.

Total cellular protein extraction and WB. Cells were collected and washed with pre-cold PBS. Their proteins were extracted by adding RIPA buffer (Beijing Solarbio Science & Technology Co., Ltd.; cat. no. R0020), supplemented with protease inhibitors (Beyotime Institute of Biotechnology; cat. no. P1010), incubated on ice for ≥30 min, and vortexed for 20 sec every 10 min. The soluble fraction was the isolated by centrifugation at 14,000 x g for 10 min at 4˚C, and the supernatant was transferred to a new tube.

For immunoblotting, total cellular proteins were subjected to quantification by using BCA Protein Assay Kit. The protein extracts were resolved by SDS-PAGE in 12% polyacrylamide (20 μg protein loaded per lane) and transferred to a 0.45-μm PVDF membrane (MilliporeSigma; cat. no. R1MB61296). Membranes were blocked with 5% non-fat dried milk in TBS containing 0.1% Tween-20 (Shandong Sparkjade Scientific Instruments Co., Ltd.; cat. no. ED0009) for 1 h at room temperature and incubated with the indicated primary antibodies overnight at 4˚C, followed by incubation with HRP-conjugated goat secondary antibodies (1:2,000) for 1 h at room temperature. The bands were analyzed using ECL Plus detecting reagents (Beijing Solarbio Science & Technology Co., Ltd.; cat. no. PE0010) and Amersham Imager 600 (Cytiva).

IF of cells in suspension. Suspended cells were collected by centrifugation at 1,000 x g for 5 min at room temperature. Next, the pellet was resuspended with 100 μl culture medium. A single-cell coating at a density of 5-$6x10^5$ cells was obtained on the slide using the Thermo Shandon Cytospin 4 machine (Thermo Fisher Scientific, Inc.) according to the manufacturer's instructions. The cells were fixed with 4% paraformaldehyde (Beyotime Institute of Biotechnology; cat. no. P0099) for 20 min at room temperature. Next, the cells were permeabilized with 0.1% Triton X-100 (Beijing Solarbio Science & Technology Co., Ltd.; cat. no. T8200) in PBS for 5 min and blocked with 5% bovine serum albumin (BSA) (Beijing Solarbio Science & Technology Co., Ltd.; cat. no. A8010) in PBS for 1 h at room temperature. The samples were incubated with anti-LC3B primary antibody in 1% BSA in PBS overnight at 4˚C. Next, the cells were washed with PBS and incubated with a secondary antibody in 1% BSA in PBS for 1 h at room temperature, followed by DAPI (10 μg/ml; Beijing Solarbio Science & Technology Co., Ltd.; cat. no. S2110) staining. The cells were then mounted using coverslips and visualized under a confocal microscope (Leica Microsystems, Inc.; cat. no. TCS SP8).

Electron microscopy. Cells were fixed in 0.2 M sodium cacodylate buffer (pH 7.4) containing 2% paraformaldehyde and 2.5% glutaraldehyde overnight at 4˚C, washed with 0.1 M sodium cacodylate buffer for 3 times at 25˚C, postfixed in 1% osmium tetroxide for 2 h at 4˚C and stained with 1% uranyl acetate overnight at 4˚C. Following stepwise ethanol and acetone dehydration, samples were infiltrated with Epon resin overnight at 60˚C. Finally, the samples were sectioned at a thickness of 70 nm and observed by transmission electron microscopy (TEM; Hitachi, Ltd.; cat. no. HT7700).

RNA-sequencing (RNA-seq) analyses. mRNA sequencing was performed using WT and *KDM3B* KO K562 cells (Shanghai GeneChem Co., Ltd.). The cells were collected after starvation in EBSS medium for 4 h before RNA was extracted. A total of 1 μg RNA per sample was used as input material for RNA sample preparations. Sequencing libraries were generated using NEBNext® Ultra™ RNA Library Prep Kit for Illumina® (New England BioLabs, Inc.) following the manufacturer's recommendations, and index codes were added to attribute sequences to each sample. The clustering of the index-coded samples was performed on a cBot Cluster Generation System using TruSeq PE Cluster Kit v3-cBot-HS (Illumina, Inc.) according to the manufacturer's instructions. After cluster generation, the library preparations were sequenced on an Illumina Novaseq platform (Illumina, Inc.), and 150-bp paired-end reads were generated. Clean data (clean reads)

were obtained by removing reads containing adapter, poly-N and general low-quality reads from raw data. At the same time, the clean data were inspected for Q20, Q30 and GC content. The sequencing process itself has the possibility of machine error, and the inspection of sequencing error rate distribution can reflect the quality of sequencing data. If the sequencing error rate is represented by e (46) and the base mass value of Illumina is represented by Q_{phred}, Q_{phred}=-10log10(e). Q20 represents the percentage of bases with a phred value higher than 20 in the population, and Q30 represents the percentage of bases with a phred value higher than 30 in the population. GC content represents the percentage of G and C in the four bases of clean reads.

All downstream analyses were based on the resulting high-quality clean data. Reference genome and gene model annotation files were downloaded from genome websites directly. Indexing of the reference genome was built using Hisat2 v2.0.5 software, and paired-end clean reads were aligned to the reference genome. Differential expression analysis of two conditions/groups was performed using the DESeq2 package (47). The resulting P-values were adjusted using Benjamini and Hochberg's approach for controlling the false discovery rate. Genes with an adjusted P<0.05 found by DESeq2 were considered to be differentially expressed. Gene Ontology (GO) enrichment analysis of differentially expressed genes was implemented via the clusterProfiler R package, in which gene length bias was corrected. GO terms with corrected P<0.05 were considered as significantly enriched by differential expressed genes. The clusterProfiler R package was used to evaluate the statistical enrichment of differential expression genes in Kyoto Encyclopedia of Genes and Genomes (KEGG) pathways.

RNA extraction, cDNA synthesis and reverse transcription-quantitative PCR (RT-qPCR) analysis. Total RNA was extracted using TRIzol® (Shandong Sparkjade Scientific Instruments Co., Ltd.), and cDNA was obtained from 2 μg total RNA by RT using the Evo M-MLV cDNA Synthesis kit (Jiangsu Accuracy Biotechnology Co., Ltd.; cat. no. AG11706) according to the manufacturer's instructions. qPCR was carried out by Applied Biosystems 7500 Fast Real-Time PCR System (Thermo Fisher Scientific, Inc.) with SYBR Green Premix Pro TaqHS qPCR Kit (Rox Plus) (Jiangsu Accuracy Biotechnology Co., Ltd.; cat. no. AG11718). The thermocycling conditions were as follows: Initial denaturation, 95˚C for 30 sec; followed by 40 cycles of denaturation (95˚C for 10 sec); annealing (55˚C for 20 sec) and extension (72˚C for 30 sec). The relative gene expression was analysed using the $2^{-\Delta\Delta Cq}$ method (48). *ACTB* was used as a control for normalization. All reactions were performed as triplicates. The following primers were used: *ACTB* forward, 5'-ATTGCCGACAGGATGCAGAA-3' and reverse, 5'-ACATCTGCTGGAAGGTGGACAG-3'; and *GABARAPL1* forward, 5'-GAATCCACCTGAGACC-3' and reverse, 5'-GCCTTACACTGCCATA-3'.

Luciferase assays. For luciferase assays, the *GABARAPL1* gene promoter regions (from ~1 kb upstream of the transcription start site to ~200 bp downstream) were amplified from genomic DNA and inserted into the pGL3.0-basic vector (Promega Corporation) by two restriction endonucleases, *Nhe*I and *Hind*III. For plasmid transfection in 293T cells, Lipofectamine® 3000 (Invitrogen; Thermo Fisher Scientific, Inc.; cat. no. L3000015) was used according to the manufacturer's instructions. Luciferase activities were measured after 48 h of transfection using a Dual-Luciferase Reporter Assay System (Promega Corporation; cat. no. E2920) according to the manufacturer's instructions, and Sirius L Tube Luminometer (Titertek-Berthold). *Renilla* luciferase activity was used as a control for normalization. Experiments were independently repeated ≥3 times. The following primers were used: *GABARAPL*1-*Nhe*I forward, 5'-CTAGCTAGCGCT TGATACTCTCTTTTCCA-3' and *GABARAPL1-Hind*III reverse, 5'-CCCAAGCTTTGACCCTGTCCCGCTCC-3'.

Chromatin immunoprecipitation (ChIP)-qPCR analysis. For ChIP assay, a kit from Beyotime Institute of Biotechnology (cat. no. P2078) was used. Briefly, cells were collected and crosslinked with 1% formaldehyde for 10 min in PBS at room temperature, followed by quenching for 5 min with 0.125 M glycine. After centrifugation at 1,000 x g for 5 min at 4˚C, the cell pellets were lysed in SDS-lysis buffer, supplemented with 1 mM PMSF (Beyotime Institute of Biotechnology, Inc.; cat. no. ST506), and sonicated. The supernatant lysates were incubated with protein A+G agarose/salmon sperm DNA (Beyotime Institute of Biotechnology, Inc.; cat. no. P2078-1) for pre-clearing, and then subjected to IP with IgG (Beyotime Institute of Biotechnology, Inc.; cat. no. A7016) and the indicated antibodies. The immunoprecipitants were washed with low-salt wash buffer, high-salt wash buffer, LiCl wash buffer and Tris-EDTA buffer before being eluted in elution buffer (1% SDS and 0.1 M NaHCO3). Next, the supernatant was incubated with 5 M NaCl for 4 h at 65˚C to reverse cross-link, and digested with 0.5 M EDTA, 1 M Tris (pH 6.5) and proteinase K for 1 h at 45˚C. DNA was purified and then analyzed by RT-qPCR. The enrichment value of bound DNA was calculated relative to the input. The following primers were used in ChIP-qPCR assay: *GABARAPL1*-P1 region forward, 5'-TGCCCTAATGCCCAATCTTC-3' and reverse, 5'-TTGGCCAATGCAGAGCTGT-3'; and *GABARAPL1*-P2 region forward, 5'-TCTGCATTGGCCAAAGGGAT-3' and reverse, 5'-TAGCTGCAGAAACGTCCGCT-3'.

Cell viability assay. Cell Counting Kit (CCK)-8 assay was used to detect cell viability. K562, THP1 and U937 cells (WT and *KDM3B* KO) were seeded into 96-well plates with $1x10^4$ cells per well. Cells were cultured for 48 h, and then 10 μl CCK-8 (Beijing Solarbio Science & Technology Co., Ltd.; cat. no. CA1210) was added to each well and incubated for 4 h at 37˚C. The total volume in each well was 100 μl. The absorbance was measured at 450 nm using a microplate reader (Thermo Fisher Scientific, Inc.).

Statistical analysis. Statistical significance was performed using unpaired Student's t-test, One-way analysis of variance (ANOVA) or Two-way ANOVA with multiple comparisons test unless otherwise stated. All statistical analyses were assessed using GraphPad Prism 9.0 (Dotmatics), unless otherwise stated. Data are presented as the mean ± SD. In all analysis,

P<0.05 was considered to indicate a statistically significant difference. All experiments were independently repeated at least three times.

The clinical data and gene expression profiles were obtained from The Cancer Genome Atlas database (https://portal.gdc.cancer.gov). The survival rate and expected survival time were used to measure disease prognosis. Survival curves were generated using the Kaplan-Meier method followed by the log-rank test. The correlation between KDM3B and GABARAPL1 was analyzed by Spearman's correlation analysis. Cox and logistic regression were used to analyze the relationship between KDM3B, GABARAPL1 expression levels and AML clinical phenotypes. Data were expressed as the median (interquartile range) or the mean ± SD for continuous variables.

Results

Loss of KDM3B decreases LC3B-II levels and inhibits autophagy in different leukemia cells. To investigate the effect of KDM3B expression on leukemia cell autophagy, the autophagic process was first analyzed in K562, THP1 and U937 cells under starvation or rapamycin stimulation by examining the conversion of LC3B-I to LC3B-II as a standard marker of autophagic activity and the decrease of the autophagic substrate SQSTM1. Western blot analysis showed that LC3B-II levels were significantly increased upon starvation or rapamycin induction in K562 cells, while the SQSTM1 levels showed an opposite trend (Fig. S1A). A similar trend was observed in THP1 and U937 cells (Fig. S1B and C).

To further explore the role of KDM3B in autophagy, four different *KDM3B* KO stable cell lines (*KDM3B* KO K562 cells, *KDM3B* KO THP1, *KDM3B* KO U937 and *KDM3B* KO 293T cells) were constructed using CRISPR/Cas9 technology (Fig. S1D). WB confirmed efficient KO in all cell lines (Fig. S1E).

CCK-8 assay was also used to measure cell viability after *KDM3B* KO. As demonstrated in Fig. S1F, compared with the WT group, the cell viability was significantly increased after *KDM3B* KO, suggesting that KDM3B expression could inhibit cell proliferation.

Next, the autophagic process was analyzed in WT and *KDM3B* KO K562 cells upon starvation induction by WB. It was observed that the LC3B-II levels were increased in WT K562 cells compared with cells under normal culture conditions. This increase was time dependent, becoming significant with increased starvation time. The SQSTM1 levels exhibited an opposite trend. However, *KDM3B* KO inhibited LC3B-II formation, while the LC3B-II and SQSTM1 levels remained stable after starvation induction (Fig. 1A).

The autophagic process was also investigated in WT and *KDM3B* KO K562 cells by rapamycin stimulation. WB revealed the accumulation of LC3B-II and the degradation of SQSTM1 in WT K562 cells upon rapamycin stimulation compared with cells under normal culture conditions. *KDM3B* KO inhibited LC3B-II formation, whereas the LC3B-II or SQSTM1 levels did not differ after rapamycin stimulation (Fig. 1B). Similar trends for LC3B-II and SQSTM1 levels were also observed in THP1 and U937 cells (Fig. 1C-F). Collectively, these results suggested that KDM3B was a critical regulator of autophagy.

KDM3B promotes autophagosome formation. To further investigate KDM3B functions in autophagy, the present study explored whether KDM3B affects autophagosome formation upon starvation induction. IF and confocal fluorescence microscopy analyses identified the formation of a LC3B-positive autophagosome upon starvation induction. First, the increase in LC3B punctate cells was notably attenuated in *KDM3B* KO cells compared with WT K562 cells (Fig. 2A). Second, TEM further showed an increase in the number of autophagic vesicles in WT K562 cells but not in *KDM3B* KO K562 cells (Fig. 2B). Under TEM, the early stage of autophagosome formation was cup shaped and had a double-membrane structure, which half enclosed the components that needed to be degraded. The complete autophagosome was a bilayer vesicle containing components that needed to be degraded. Autophagosomes were generally 300-900 nm in size, with a mean size of 500 nm. These results indicated that KDM3B played a role in promoting autophagosome formation.

KDM3B-associated autophagy flux. To investigate the KDM3B-associated autophagy process, the KDM3B-involved autophagy flux was evaluated via *KDM3B* KO. Western blot analysis showed that *KDM3B* KO inhibited LC3B-II formation in K562 upon starvation induction (Figs. 1, and 3A and B). In addition, LC3B-II accumulated during BafA1 treatment, and the autophagic substrate SQSTM1 level exhibited a corresponding change with LC3B-II (Fig. 3A). Consistent results were observed in THP1 cells (Fig. 3B).

Autophagy flux tests were performed using a tandem fluorescent indicator, mCherry-GFP-LC3B, in *KDM3B* KO and WT 293T cells upon starvation induction. Since the green fluorescence of the fusion protein is sensitive in lysosomes and quickly quenched in autolysosomes, only red fluorescence could be detected in autolysosomes. Therefore, results showing yellow or green puncta indicate the presence of autophagosomes. Fluorescence analysis using the aforementioned tandem fluorescent indicator system showed that *KDM3B* KO significantly inhibited the formation of autophagosomes compared with WT 293T cells upon starvation. Under normal conditions, there was no significant difference between *KDM3B* KO and WT 293T cells. However, further starvation and BafA1 combined treatment showed a significant accumulation of autophagosomes in WT 293T but not in *KDM3B* KO 293T cells (Fig. 3C and D). These results suggested that KDM3B promoted autophagosome formation and functioned as a factor in autophagy flux.

KDM3B regulates the expression of GABARAPL1, which is involved in the process of autophagy. To explore the mechanism of KDM3B in the transcriptional regulation of autophagy, RNA-seq was performed in WT and *KDM3B* KO K562 cells after starvation treatment. A total of 1,105 differentially expressed genes were found (Fig. 4A and B). KEGG analysis was performed for all the downregulated genes after *KDM3B* KO in K562 cells. The top 20 signaling pathways are shown in Fig. 4C. Among them, the PI3K-Akt and lysosomal signaling pathways were closely associated the regulation of autophagy.

GABARAPL1, an autophagy-related gene, was identified among all the downregulated genes through analysis using volcano plots (Fig. 4D). The KDM3B dependency of the

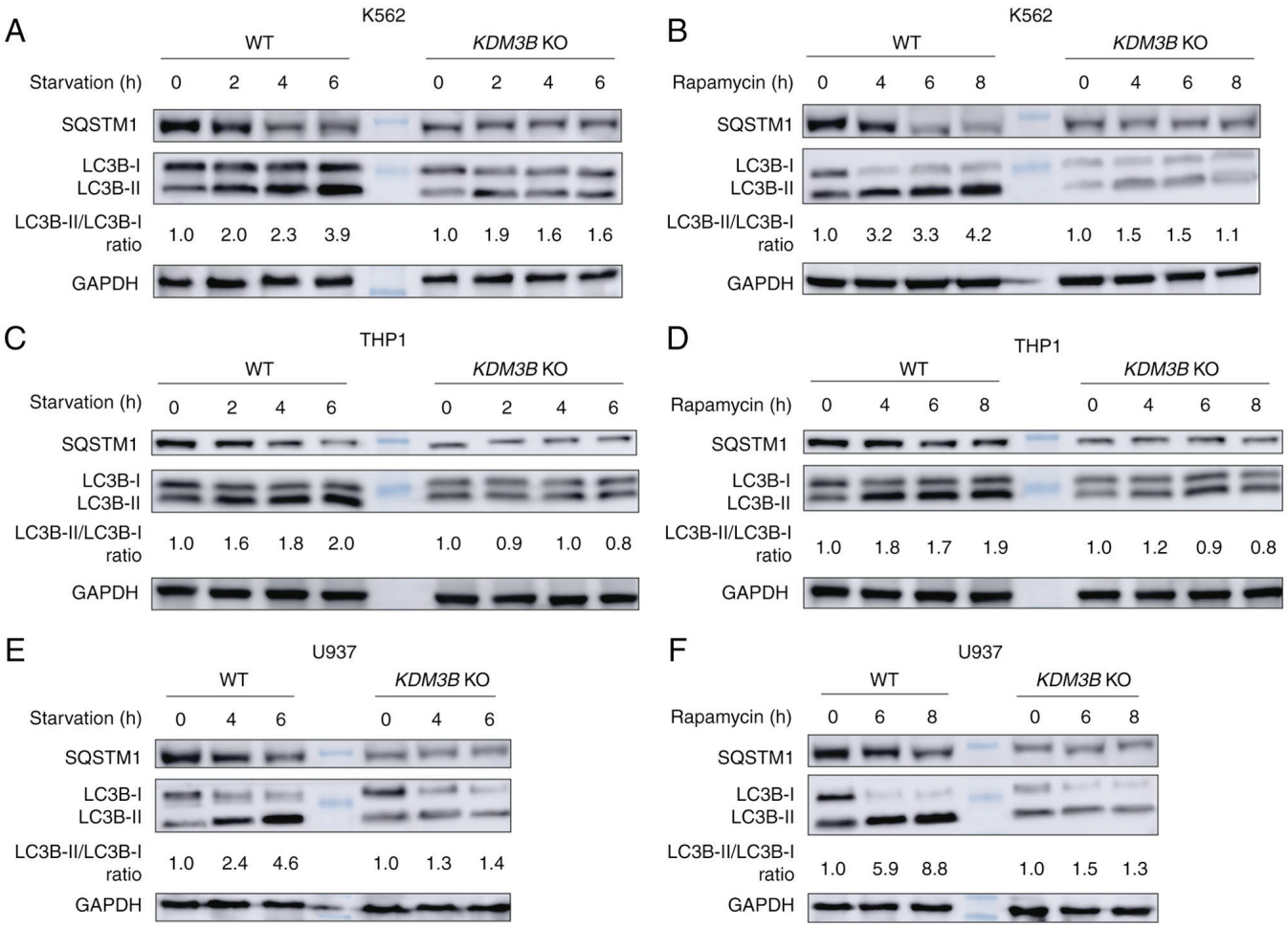

Figure 1. The expression of KDM3B is critical for autophagy. *KDM3B* KO decreased autophagy. (A and B) WT or *KDM3B* KO K562 cells were cultured in the starvation EBSS medium (A) or treated with rapamycin (5 μM) (B) for the indicated times. (C and D) WT or *KDM3B* KO THP1 cells were cultured in the starvation EBSS medium (C) or treated with rapamycin (5 μM) (D) for the indicated times. (E and F) WT or *KDM3B* KO U937 cells were cultured in the starvation EBSS medium (E) or treated with rapamycin (5 μM) (F) for the indicated times. Cell lysates were analyzed by immunoblotting with the anti-SQSTM1, anti-LC3B, and anti-GAPDH antibodies. GAPDH was used as an endogenous control. The LC3B-II/LC3B-I ratio was indicated. KDM3B, histone lysine demethylase 3B; KO, knockout; WT, wild-type; EBSS, Earle's Balanced Salt Solution.

GABARAPL1 gene was validated by RT-qPCR. Three cell lines, K562, THP1 and U937 cells (WT and *KDM3B* KO), were cultured under normal and EBSS conditions (Fig. 5A) or subjected to rapamycin treatment (Fig. 5B), and the mRNA expression of *GABARAPL1* was quantified through qPCR. The results showed that the mRNA expression of *GABARAPL1* was increased in WT cell lines upon starvation or rapamycin induction compared with cell lines under normal culture conditions. However, the mRNA expression of *GABARAPL1* did not increase in *KDM3B* KO cell lines, which was consistent with the results of RNA-seq. This result suggested that KDM3B may be involved in the regulation of the *GABARAPL1* gene, which participates in the autophagic process.

KDM3B is associated with the promoter of the GABARAPL1 gene. The present study focused on *GABARAPL1* for additional analysis. To examine the KDM3B-dependent epigenetic regulation of *GABARAPL1*, two possible promoter regions for KDM3B association were mapped in the ChIP experiment (Fig. 6A). WT K562 cells were starved in an EBSS medium for 4 h and then used for ChIP assay. Agarose gel electrophoresis showed a significant binding of KDM3B to the -1,119 to -360 region (P1 region) of the *GABARAPL1* promoter compared with the -374 to +155 region (P2 region) (Fig. 6B). The efficiency of IP was evaluated by WB. As demonstrated in Fig. 6B, the data suggested that the added anti-KDM3B antibody successfully precipitated the KDM3B protein in cells. The ChIP-qPCR experiment also confirmed the recruitment of KDM3B to the -1,119/-360-*GABARAPL1*-promoter (Fig. 6C).

Next, a luciferase assay was performed to confirm the KDM3B-mediated regulation of *GABARAPL1* at the transcriptional level. A luciferase vector containing the promoter region of *GABARAPL1* was transiently overexpressed in WT and KDM3B KO 293T cells (Fig. 6D). A significant increase in luciferase signal was observed in WT 293T cells compared with *KDM3B* KO 293T cells, indicating that certain functional regulatory elements by KDM3B existed in this region. The data showed that KDM3B expression could regulate the transcription of *GABARAPL1*. In summary, these results indicated that KDM3B-dependent chromatin modifications occurred in *GABARAPL1*, which was involved in the autophagic process. Therefore, KDM3B could bind to the promoter of *GABARAPL1* and activate its transcription.

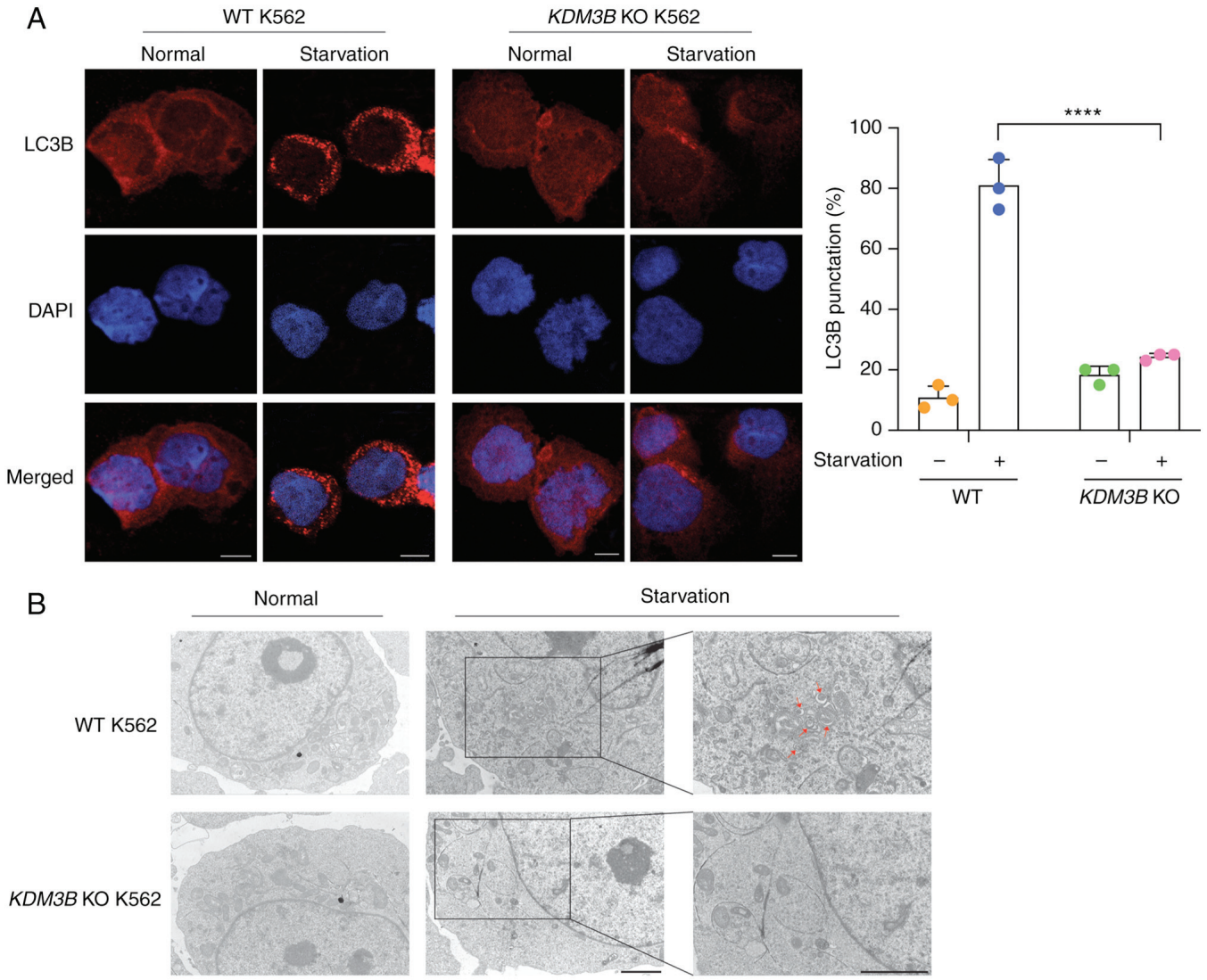

Figure 2. Expression of KDM3B promotes the formation of autophagosome. (A) Representative confocal images of endogenous LC3B puncta formation. WT or *KDM3B* KO K562 cells were cultured in the normal or EBSS medium for 4 h. A total of 10 confocal images with an average of 20 cells were used for counting LC3B-positive punctate cells in every group. Quantification of LC3B-positive punctate cells was shown on the right panels. Nuclei were counterstained with DAPI. Data (mean ± SD) were analyzed with Student's t-test. ****P<0.0001. Scale bar, 10 μm. (B) Representative TEM images of autophagosome. WT or *KDM3B* KO K562 cells were cultured in the normal or EBSS medium for 4 h. High magnification of boxed areas is shown on the right. More than 10 cells were randomly observed and their images were used for TEM data in every group. Scale bar, 2 μm. Autophagosomes with unique double membrane display (red arrowheads). KDM3B, histone lysine demethylase 3B; WT, wild-type; KO, knockout; TEM, transmission electron microscopy; EBSS, Earle's Balanced Salt Solution.

Re-expression of WT KDM3B rescues GABARAPL1 expression and autophagy. To clarify if KDM3B is necessary for autophagy, WT KDM3B (Flag-tagged) was re-expressed in *KDM3B* KO 293T cells. WB showed that the LC3B-II levels were increased in WT 293T cells upon starvation induction compared with normal culture conditions. The SQSTM1 levels exhibited the opposite trend. However, *KDM3B* KO inhibited LC3B-II formation, and the LC3B-II or SQSTM1 levels did not differ during starvation induction. When KDM3B expression was rescued in *KDM3B* KO 293T cells, prominent LC3B-II formation reappeared under starvation conditions, and SQSTM1 exhibited an opposite trend (Fig. S2A).

RT-qPCR was used to confirm the mRNA expression of *GABARAPL1* in 293T cells. The results demonstrated that the *GABARAPL1* mRNA expression was increased in WT 293T cells upon starvation induction compared with normal culture conditions, but not in *KDM3B* KO 293T cells. When KDM3B expression was rescued in *KDM3B* KO 293T cells, it could promote *GABARAPL1* expression (Fig. S2B). Finally, WT or *KDM3B* KO 293T and K562 cells were used to evaluate the GABARAPL1 protein expression levels. Western blot analysis showed that the GABARAPL1 levels were increased in WT cells after stimulation compared with normal culture conditions. *KDM3B* KO inhibited GABARAPL1 expression (Fig. S2C and D). GABARAPL1 levels recovered when KDM3B expression was rescued in *KDM3B* KO 293T cells (Fig. S2C). Re-expression of WT KDM3B in *KDM3B* KO 293T cells also rescued the luciferase activity (Fig. 6D). Collectively, these data indicated that KDM3B was a crucial molecule in autophagy and functioned by increasing the expression of GABARAPL1.

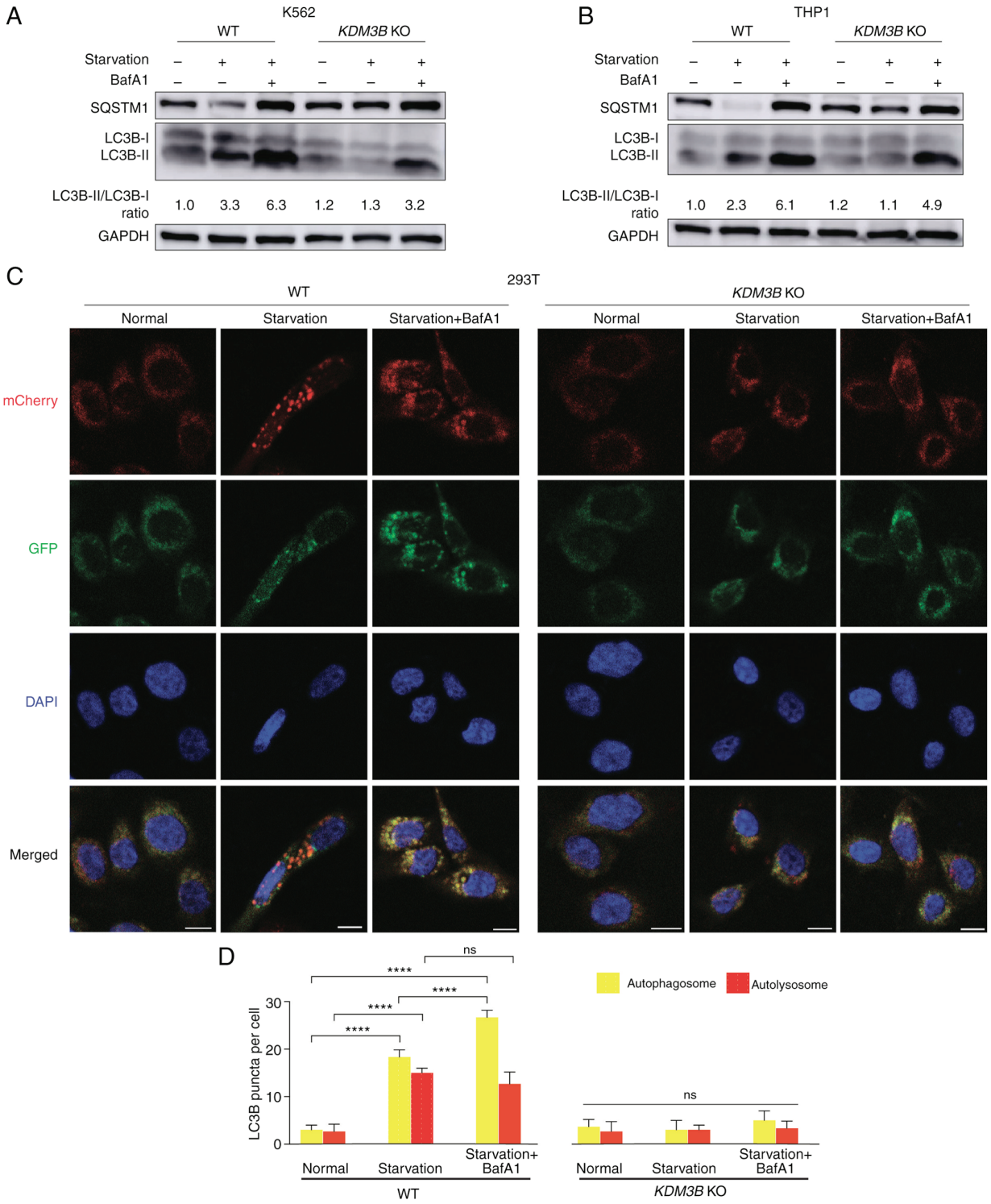

Figure 3. Defects in autophagic flux caused by the loss of KDM3B. (A and B) LC3B flux was analyzed in WT and *KDM3B* KO K562 cells (A) or THP1 cells (B) in the absence or presence of BafA1 (100 nM, 2 h). Cells were cultured and then starved in EBSS (4 h) with or without BafA1. *KDM3B* KO inhibited LC3B-II formation. BafA1 treatment resulted in the accumulation of LC3B-II and SQSTM1. The LC3B-II/LC3B-I ratio is indicated. (C) Autophagy flux was revealed by the mCherry-GFP-LC3 tandem reporter. The plasmid was transfected in WT or *KDM3B* KO 293T cells. Representative images of the cells cultured in normal, EBSS medium (4 h) or EBSS with BafA1 (100 nM) addition (2 h), respectively. Moreover, the formation of autophagosome (yellow: mCherry-positive; GFP-positive) and autolysosome (red: mCherry-positive; GFP-negative) was examined. Scale bar, 10 μm. (D) Statistical analysis of vesicles positive for both GFP and mCherry (autophagosomes) and for mCherry (autolysosomes) (>20 cells per experiment) in (C) Data (mean ± SD) were analyzed with two-way ANOVA. ns, not significant; ****P<0.0001. KDM3B, histone lysine demethylase 3B; WT, wild-type; KO, knockout; BafA1, bafilomycin A1; EBSS, Earle's Balanced Salt Solution.

Identification of the correlation between KDM3B and GABARAPL1. The occurrence of leukemia is closely related to the dysfunction of autophagy. In addition to exploring the role of KDM3B in autophagy in AML cell lines, the information of patients' samples from the online public database (https://portal.gdc.cancer.gov) was also analyzed to reveal

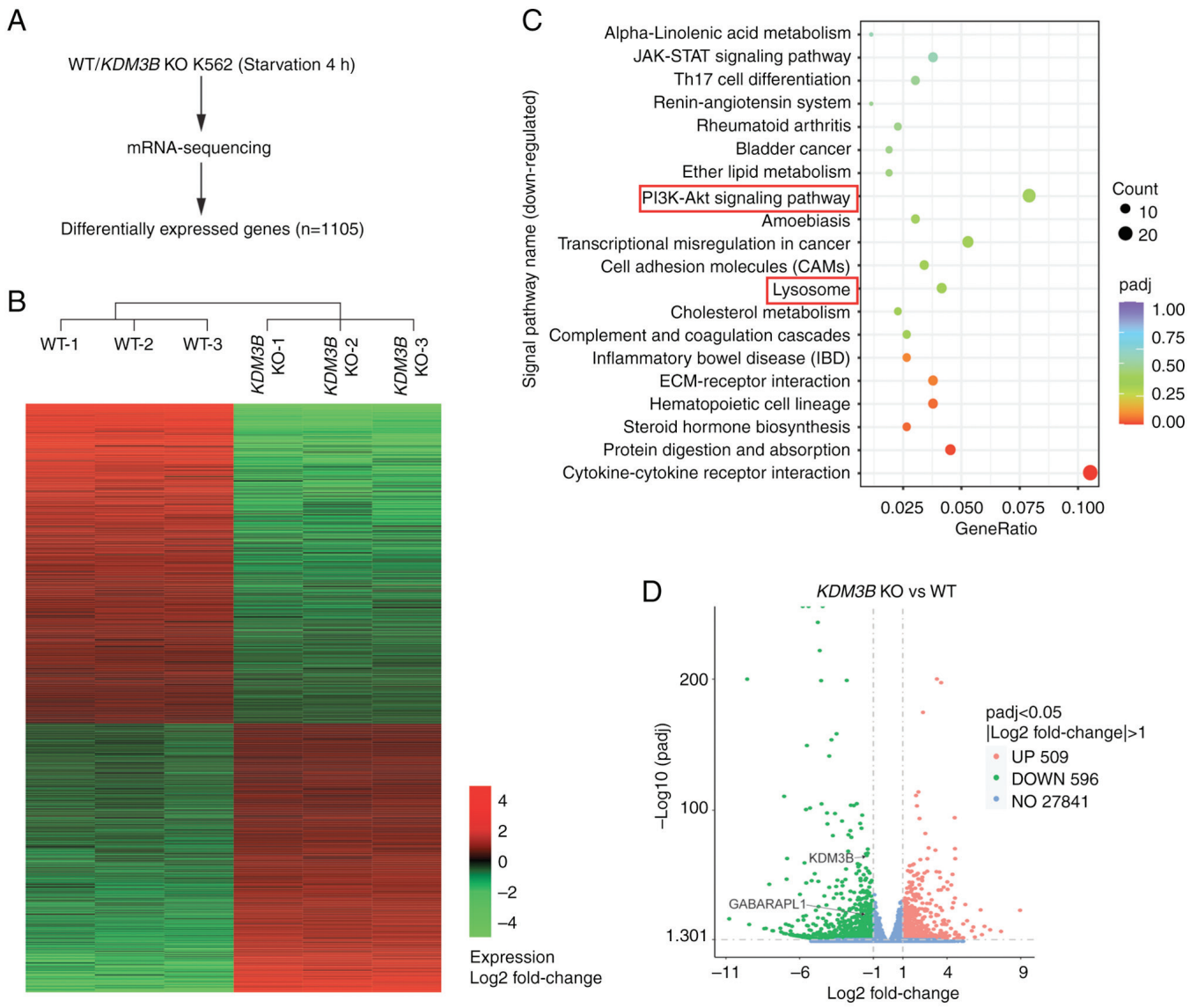

Figure 4. Identification of KDM3B target genes by RNA-seq analysis. (A) Flow chart showing the strategy of RNA-seq. (B) Hierarchical clustering results applied to 1,105 differentially expressed genes. (C) Kyoto Encyclopedia of Genes and Genomes pathway analyses of all downregulated genes after *KDM3B* KO in K562 cells. (D) Volcano plots indicated the differentially expressed genes. Red dots represented upregulated genes, green dots represented downregulated genes, and blue dots represented equally expressed genes. KDM3B and GABA type A receptor-associated protein like 1 were indicated with black arrows. KDM3B, histone lysine demethylase 3B; RNA-seq, RNA sequencing; KO, knockout; WT, wild-type.

the expression changes of KDM3B and GABARAPL1 in normal controls and patients with AML, and the relationship between expression levels and patient survival was analyzed. According to the data analysis, increased KDM3B and GABARAPL1 gene expressions were both associated with favorable outcomes of the patients (Fig. S3A and B). Lower KDM3B and GABARAPL1 expression levels were determined in patients with AML compared with normal controls (Fig. S3C). Furthermore, a positive correlation between KDM3B and GABARAPL1 expression was identified in AML patients (Fig. S3D). In addition, multiple regression analyses (Fig. S4) were performed to detect the association between KDM3B, GABARAPL1 expression levels and certain AML clinical variables. The results indicated that, like the majority of other clinical phenotypes, the KDM3B (HR=0.711, P=0.102) and GABARAPL1 (HR=0.944, P=0.591) expression levels could not independently predict AML prognosis. These results suggested that KDM3B and GABARAPL1 may interact with other clinical variables and be beneficial to the prognosis of AML. Hence, logistic regression analysis (Fig. S5) was performed and the results suggested that a low expression of KDM3B correlated with FAB classifications (OR=0.423, P=0.013). GABARAPL1 expression correlated not only with FAB classifications (OR=3.421, P<0.001), but also with BM blasts (OR=0.262, P<0.001). But neither was associated with certain common gene mutations, including nucleophosmin 1 (NPM1), and fms related receptor tyrosine kinase 3 (FLT3).

Discussion

Autophagy is a relatively conserved multistep degradation process of intracellular components. The activation of the ULK1 complex and PI3K complex 1 (PtdIns3K-C1) causes

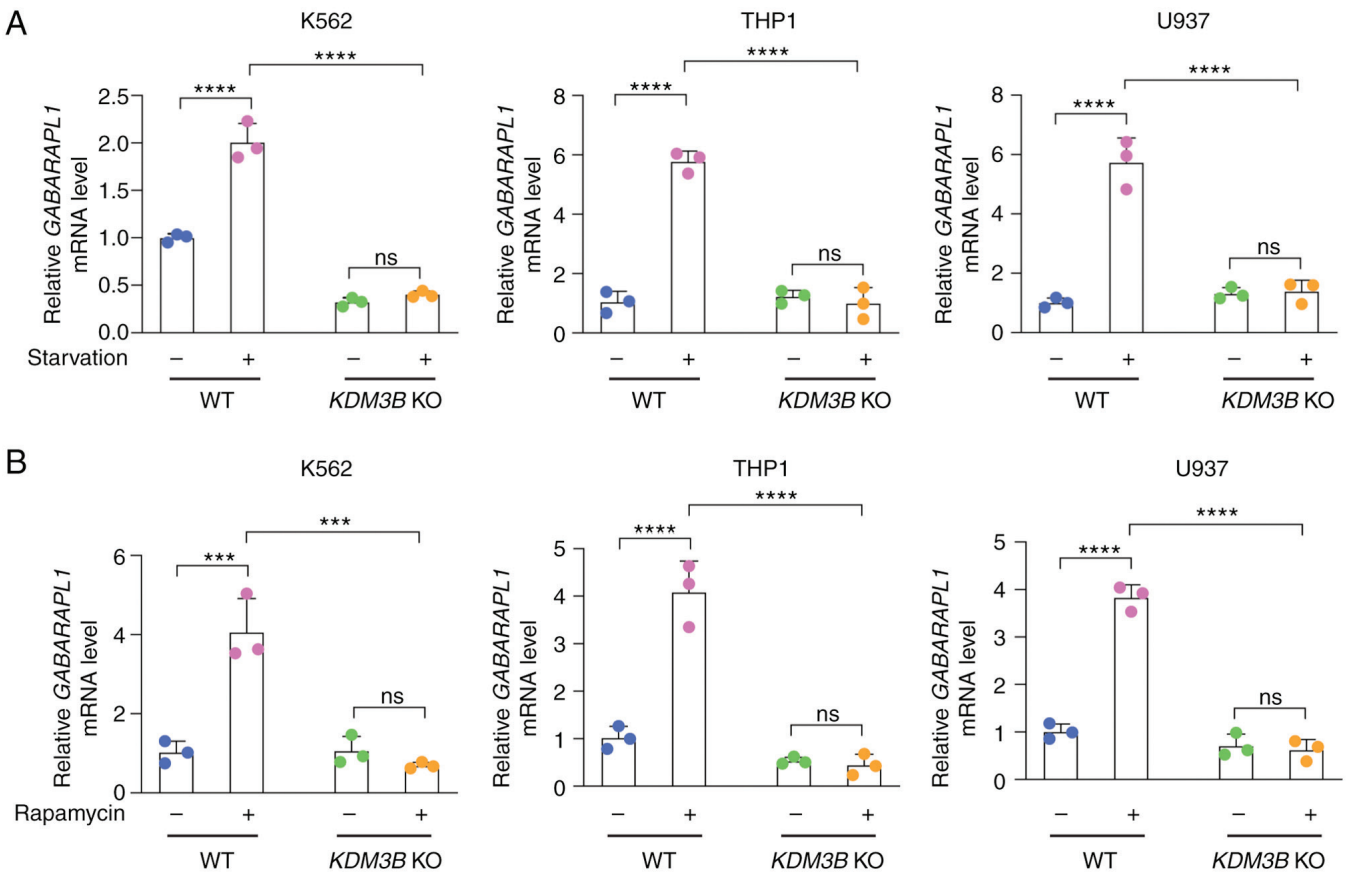

Figure 5. KDM3B deficiency leads to decreased expression of *GABARAPL1*. (A and B) Reverse transcription-quantitative PCR analysis of KDM3B-dependent autophagy-related gene *GABARAPL1* in K562, THP1 or U937 cells. Cells were cultured and then starved in Earle's Balanced Salt Solution for 4 h (A) or treated with rapamycin (5 μM) for 4 h (B) Data (mean ± SD) were analyzed with two-way ANOVA. ns, not significant; ***P<0.001 and ****P<0.0001. KDM3B, histone lysine demethylase 3B; GABARAPL1, GABA type A receptor-associated protein like 1; KO, knockout; WT, wild-type.

vesicle nucleation and initiates autophagosome formation (49,50). GABARAPL1 plays a vital role in the initiation of autophagy. It participates in the re-localization of ULK1 to the phagophore, and regulates the activation and phosphorylation of ULK1 (51). The assembled ULK1 complex can also recruit and activate PtdIns3K-C1 together with GABARAPL1 (52,53). GABARAPL1 is more likely to be involved in closure than elongation during the extension and closure stages from the phagophore. By contrast, LC3B is more involved in the extension stage (54). Therefore, LC3 deficiency leads to the formation of smaller autophagosomes, while GABARAP deficiency results in larger autophagosomes. The final step of autophagy is the fusion of the autophagosome and lysosome, which includes the transport of the autophagosome to the lysosome through the microtubule skeleton before the fusing process. Previous studies showed that LC3B was more prone to autophagosome re-localization (55,56), while GABARAPL1 was more involved in the fusion process and could also help to increase the number of available lysosomes to ensure the regular progress of autophagy (57,58). Notably, a previous study has shown that LC3B can assist with the fusion process in cells lacking GABARAPLs (59).

Although there are partial functional compensations between GABARAP and LC3 subfamily members, the focus of each member's function is different. Controversies exist about their expression patterns and roles in different cancer types. Certain studies have found that the expression of Gabarapl1 in rat brains is significantly higher than that of other Atg8 family members (60,61). This observation suggests that Gabarapl1 may have a role in regulating central nervous system functions, such as the regulatory association between autophagy and numerous neurodegenerative diseases. In addition, Gabarapl1 is highly expressed in the hypothalamus and is regulated by estrogen. The hypothalamus contains the signaling pathway regulating male and female reproduction, revealing another potential function of Gabarapl1 in addition to autophagy regulation. Given the importance of these members, targeted studies on their expression and regulation patterns are of great importance in identifying effective treatments for different types of cancer.

Among the types of leukemia within the focus of the present study, published studies on KDM3B and GABARAPL1 are relatively rare. A previous study showed that microRNA (miR)-15a-5p was highly expressed in patients with chemoresistant AML, and miR-15a-5p downregulated the expression of four autophagy-related genes, namely ATG9a, ATG14, GABARAPL1 and sphingomyelin phosphodiesterase 1, which further inhibited autophagy and eliminated the therapeutic effect of daunorubicin-induced autophagy (62). KDM3B, which was initially considered a tumor suppressor gene, is located in the region of chromosome 5q31, which is often absent in abnormal bone marrow development and AML (33).

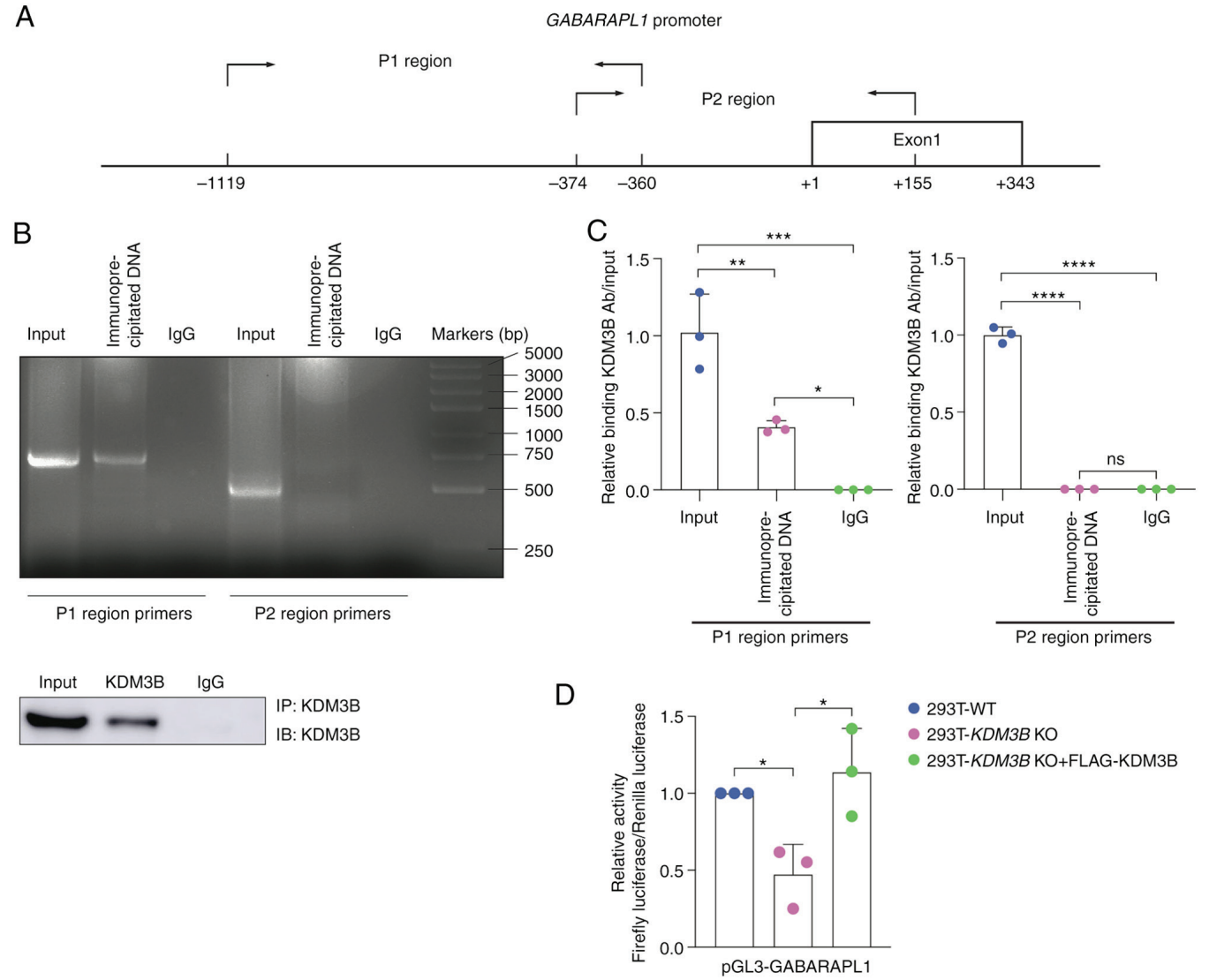

Figure 6. Depletion of KDM3B alters KDM3B promoter binding of *GABARAPL1*. (A) Schematic diagram of primer relative positions (P1 region and P2 region) on the *GABARAPL1* gene promoter used for (B) and (C). (B) ChIP assay. Upper, sonicated chromatin from WT K562 cells starved in EBSS (4 h) was immunoprecipitated with anti-KDM3B or preimmune IgG (control). Agarose gel electrophoresis showed that a fragment corresponding to the -1119 to -360 region (P1 region) of *GABARAPL1* promoter was amplified using the immunoprecipitated DNA as a template. Below: Western blot analysis of KDM3B in the immunoprecipitated samples, followed by immunoblotting with the anti-KDM3B antibody. A total protein of 20 μg was added into each well for western blot analysis. (C) Quantitative PCR of ChIP analysis revealed that KDM3B can bind to the *GABARAPL1* gene promoter (P1 region) *in vivo*. The data were normalized by input. (D) Luciferase assays. WT, *KDM3B* KO or *KDM3B*-rescued 293T cells were transiently transfected with pGL3.0-*GABARAPL1* promoter. Luciferase activities were measured followed by EBSS medium for 4 h. Data (mean ± SD) were analyzed with one-way ANOVA. ns, not significant; *P<0.05, **P<0.01, ***P<0.001 and ****P<0.0001. KDM3B, histone lysine demethylase 3B; GABARAPL1, GABA type A receptor-associated protein like 1; ChIP, chromatin immunoprecipitation; WT, wild-type; KO, knockout; EBSS, Earle's Balanced Salt Solution.

Analysis of patients with AML showed that KDM3B underexpression was associated with poor prognosis, while KDM3B downregulation promoted the proliferation of NB4 cells. After treatment of NB4 cells with all-trans retinoic acid, KDM3B promoted promyelocytic leukemia/retinoic acid receptor α fusion protein degradation, thereby promoting NB4 differentiation into mature granulocytes (63). However, it has also been reported that KDM3B is upregulated in patients with acute lymphoblastic leukemia, and inhibits the all-trans retinoic acid-induced differentiation of HL-60 cells (44).

The present study showed that genetic depletion of the histone lysine demethylase KDM3B attenuated the level of LC3B-II, suppressed autophagosome formation and increased the accumulation of SQSTM1. Furthermore, the expression of KDM3B ensured autophagy flux under stress conditions. The current data suggested that KDM3B regulated the expression of GABARAPL1, which was involved in autophagy at the transcriptional level via associating with the target gene promoter, leading to increased transcription of GABARAPL1 during the autophagic process (Fig. 7). Subsequently, GABARAPL1 participated in different stages of autophagy, including the recruitment and activation of the complex at the initiation stage, and the fusion process at the later stage. The present RNA-seq results showed the effect of KDM3B KO on autophagy in the leukemia cell line K562 under autophagy induction conditions. Among all the downregulated genes, multiple candidates associated with autophagy were found. However, after further validation of the candidates using RT-qPCR (data

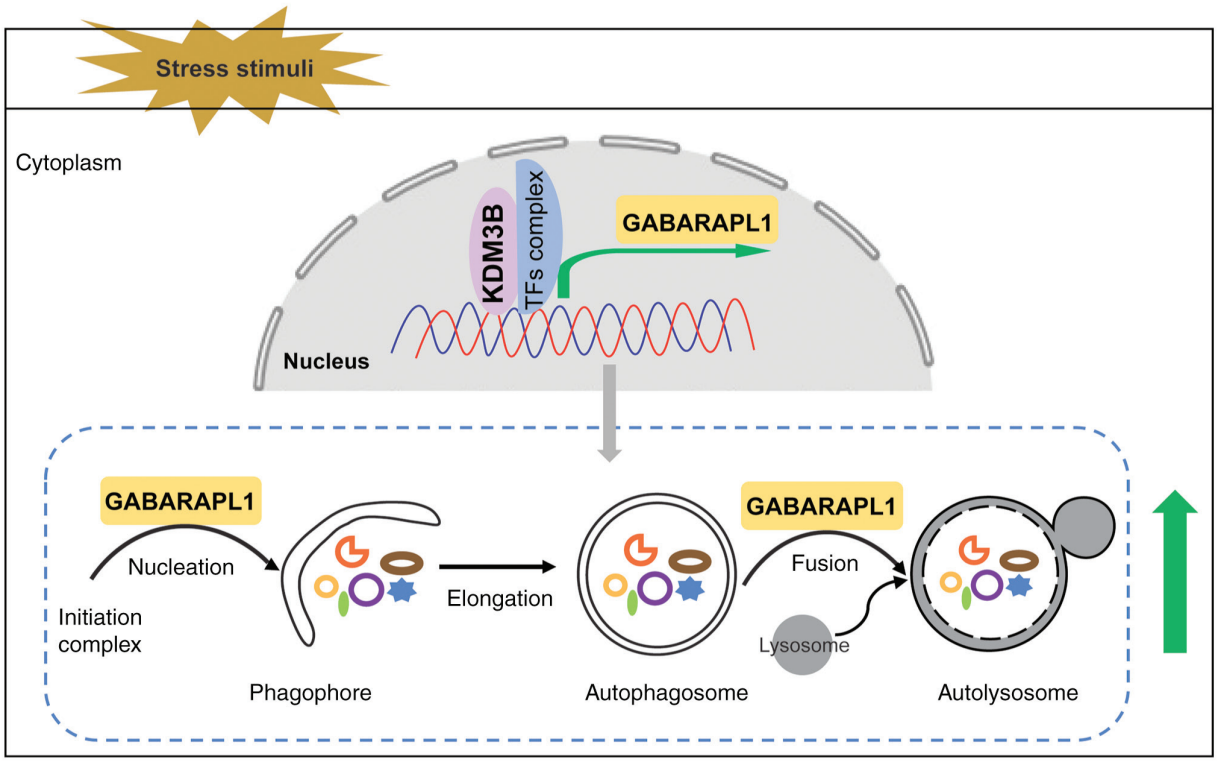

Figure 7. Graphic illustration of KDM3B promoting autophagy through increasing GABARAPL1 expression. The proposed model describes the role of KDM3B in the transcriptional and epigenetic regulation of autophagy. Under the induction of external stimuli, KDM3B binds to the promoter region of GABARAPL1 and participates in the initiation of GABARAPL1 gene transcription together with the corresponding transcription factor complex. Then GABARAPL1 protein participates in the regulation of autophagy pathway at different stages in the cytoplasm, which ensures the normal process of autophagy in leukemia cells. KDM3B, histone lysine demethylase 3B; GABARAPL1, GABA type A receptor-associated protein like 1.

not shown), GABARAPL1 was finally identified as a promising gene related to autophagy. In a previous study, RNA-seq was also conducted on HepG2 cells with KDM3B KO (64) but no GABARAPL1 was found. This difference may be due to different sequencing methods or sample sources, as different cancer cell types have different patterns in gene expression. To more comprehensively analyze the influence of KDM3B KO on downstream target genes, candidate genes identified by other studies should be further verified in leukemia cells in subsequent experiments.

The present study also focused on screening signaling pathways that may be related to autophagy. After KDM3B KO, the PI3K-Akt and lysosome-related signaling pathways were found in the top 20 downregulated pathways closely associated with autophagy in cells. This finding further supported the notion that KDM3B may be involved in the regulation of autophagy. The aforementioned two pathways played important roles in the initial formation stage and late maturation stage of autophagy, respectively. GABARAPL1 also played a vital role in the formation stage of autophagosomes and the fusion stage with lysosomes. These results indicated that KDM3B regulated GABARAPL1 expression through transcription, affecting signaling pathways and autophagy. More detailed regulatory mechanisms need to be verified in the future.

In addition, the current WB results showed that the H3K9me2 and H4R3me2s levels were decreased in WT cells after stimulation compared with normal culture conditions. KDM3B KO inhibited such observations. Therefore, it was hypothesized that KDM3B affected the histone methylation level, changed the density and accessibility of chromosomes, and facilitated the binding of the transcriptional complex. However, this hypothesis needs to be further verified through targeted experiments. A previous study found that GABARAPL1 expression in breast cancer was affected by DNA methylation, histone deacetylation and the transcription factor (cAMP response element binding protein-1 (CREB-1) (65). Although KDM3B is an important histone demethylase regulating the expression of GABARAPL1, whether it accomplishes this through interaction with transcription factors such as CREB-1 requires further investigation. The present results revealed that GABARAPL1 expression was reduced after KDM3B KO. The current RNA-seq results revealed that the upregulated signaling pathways after KDM3B knockdown included the Wnt signaling pathway (data not shown). A previous study indicated that GABARAPL1 could act as a tumor suppressor and negatively regulate the Wnt/β-catenin signaling pathway through autophagy degradation of Dishevelled (66), which is consistent with the present results. Wnt signaling plays a vital role in cell polarity and development in embryonic stem cells. It has been reported that KDM3A/B directly interacts with β-catenin in colon cancer cells and transcriptionally regulates downstream target genes in the Wnt/β-catenin signaling pathway. It affects H3/H4 histone acetylation levels, and regulates the occurrence and development of colon cancer (36). The current study did not produce sufficient experimental evidence to conclude whether KDM3B can affect the Wnt signaling pathway by regulating GABARAPL1 or autophagy, or via other mechanisms. Further studies are necessary to yield more

supporting evidence and potentially propose a new avenue for treating leukemia and other cancer types. According to the results of the present bioinformatics analysis, KDM3B was positively correlated with GABARAPL1 expression in AML. The expression levels of KDM3B and GABARAPL1 in AML were lower than normal controls, but neither of them can exist as independent prognostic factors. Therefore, more related factors need to be discovered in future studies to provide more references for the treatment of the disease.

In conclusion, the current study revealed that KDM3B regulated GABARAPL1 as an epigenetic regulator involved in autophagy in leukemia cells under stimulation. The data suggested that KDM3B, as a new candidate regulator for autophagy, increased autophagy in leukemia cells. The present findings elucidated the mechanism that KDM3B employed to regulate autophagy as an epigenetic regulator within leukemia cells, and may shed light on developing epigenetic therapeutics for leukemia and different types of cancer. One of the limitations of the present study is the lack of clinical data from AML patients; further study using clinical samples from AML patients will be undertaken in the upcoming project. Future studies are warranted to uncover the association between cell survival and autophagy caused by KDM3B in leukemia. Understanding these mechanisms could reveal novel insights for exploring the association between autophagy, cell survival, and KDM3B epigenetic regulation in leukemia and other types of cancer.

Acknowledgements

The authors would like to thank professor Xin Xu (Weifang Medical University) for critical reading of the manuscript and Dr Junfeng Shi (Affiliated Hospital of Weifang Medical University) for helping with RNA-seq analysis.

Funding

The present study was supported by the Shandong Provincial Natural Science Foundation of China (grant nos. ZR2021QH001 and ZR2020KC016) and the Weifang Science and Technology Bureau (grant no. 2020YQFK013).

Availability of data and materials

The datasets used and/or analyzed during the current study are available from the corresponding author on reasonable request.

Authors' contributions

YS designed and performed the research, analyzed the data and wrote the manuscript. JQZ performed cell cultures and related western blots. HHW performed molecular experiments. HYW and YL helped in the analysis of data. ZBH supervised the project and revised the manuscript. HYW and YL confirm the authenticity of all the raw data. All the authors have read and approved the final manuscript.

Ethics approval and consent to participate

Not applicable.

Patient consent for publication

Not applicable.

Competing interests

The authors declare that they have no competing interests.

References

1. Leidal AM, Levine B and Debnath J: Autophagy and the cell biology of age-related disease. Nat Cell Biol 20: 1338-1348, 2018.
2. Ariosa AR and Klionsky DJ: Autophagy core machinery: Overcoming spatial barriers in neurons. J Mol Med (Berl) 94: 1217-1227, 2016.
3. Yang Y and Klionsky DJ: Autophagy and disease: Unanswered questions. Cell Death Differ 27: 858-871, 2020.
4. Gatica D, Chiong M, Lavandero S and Klionsky DJ: Molecular mechanisms of autophagy in the cardiovascular system. Circ Res 116: 456-467, 2015.
5. Kimmelman AC: The dynamic nature of autophagy in cancer. Genes Dev 25: 1999-2010, 2011.
6. Condello M, Pellegrini E, Caraglia M and Meschini S: Targeting autophagy to overcome human diseases. Int J Mol Sci 20: 725, 2019.
7. Takamura A, Komatsu M, Hara T, Sakamoto A, Kishi C, Waguri S, Eishi Y, Hino O, Tanaka K and Mizushima N: Autophagy-deficient mice develop multiple liver tumors. Genes Dev 25: 795-800, 2011.
8. Capparelli C, Guido C, Whitaker-Menezes D, Bonuccelli G, Balliet R, Pestell TG, Goldberg AF, Pestell RG, Howell A, Sneddon S, *et al*: Autophagy and senescence in cancer-associated fibroblasts metabolically supports tumor growth and metastasis via glycolysis and ketone production. Cell Cycle 11: 2285-2302, 2012.
9. He S, Zhao Z, Yang Y, O'Connell D, Zhang X, Oh S, Ma B, Lee JH, Zhang T, Varghese B, *et al*: Truncating mutation in the autophagy gene UVRAG confers oncogenic properties and chemosensitivity in colorectal cancers. Nat Commun 6: 7839, 2015.
10. Takahashi Y, Coppola D, Matsushita N, Cualing HD, Sun M, Sato Y, Liang C, Jung JU, Cheng JQ, Mule JJ, *et al*: Bif-1 interacts with Beclin 1 through UVRAG and regulates autophagy and tumorigenesis. Nat Cell Biol 9: 1142-1151, 2007.
11. Elzinga BM, Nyhan MJ, Crowley LC, O'Donovan TR, Cahill MR and McKenna SL: Induction of autophagy by Imatinib sequesters Bcr-Abl in autophagosomes and down-regulates Bcr-Abl protein. Am J Hematol 88: 455-462, 2013.
12. Goussetis DJ, Gounaris E, Wu EJ, Vakana E, Sharma B, Bogyo M, Altman JK and Platanias LC: Autophagic degradation of the BCR-ABL oncoprotein and generation of antileukemic responses by arsenic trioxide. Blood 120: 3555-3562, 2012.
13. Wang Z, Cao L, Kang R, Yang M, Liu L, Zhao Y, Yu Y, Xie M, Yin X, Livesey KM and Tang D: Autophagy regulates myeloid cell differentiation by p62/SQSTM1-mediated degradation of PML-RARalpha oncoprotein. Autophagy 7: 401-411, 2011.
14. Isakson P, Bjoras M, Boe SO and Simonsen A: Autophagy contributes to therapy-induced degradation of the PML/RARA oncoprotein. Blood 116: 2324-2331, 2010.
15. Mortensen M, Soilleux EJ, Djordjevic G, Tripp R, Lutteropp M, Sadighi-Akha E, Stranks AJ, Glanville J, Knight S, Jacobsen SE, *et al*: The autophagy protein Atg7 is essential for hematopoietic stem cell maintenance. J Exp Med 208: 455-467, 2011.
16. Cao Y, Cai J, Zhang S, Yuan N, Fang Y, Wang Z, Li X, Cao D, Xu F, Lin W, *et al*: Autophagy sustains hematopoiesis through targeting notch. Stem Cells Dev 24: 2660-2673, 2015.
17. Wu F, Chen Z, Liu J and Hou Y: The Akt-mTOR network at the interface of hematopoietic stem cell homeostasis. Exp Hematol 103: 15-23, 2021.
18. Man N, Tan Y, Sun XJ, Liu F, Cheng G, Greenblatt SM, Martinez C, Karl DL, Ando K, Sun M, *et al*: Caspase-3 controls AML1-ETO-driven leukemogenesis via autophagy modulation in a ULK1-dependent manner. Blood 129: 2782-2792, 2017.

19. Settembre C, Di Malta C, Polito VA, Garcia Arencibia M, Vetrini F, Erdin S, Erdin SU, Huynh T, Medina D, Colella P, *et al*: TFEB links autophagy to lysosomal biogenesis. Science 332: 1429-1433, 2011.
20. Shin HJ, Kim H, Oh S, Lee JG, Kee M, Ko HJ, Kweon MN, Won KJ and Baek SH: AMPK-SKP2-CARM1 signalling cascade in transcriptional regulation of autophagy. Nature 534: 553-557, 2016.
21. Polager S, Ofir M and Ginsberg D: E2F1 regulates autophagy and the transcription of autophagy genes. Oncogene 27: 4860-4864, 2008.
22. Wang K, Liu JD, Deng G, Ou ZY, Li SF, Xu XL, Zhang MJ, Peng XQ and Chen FH: LncSIK1 enhanced the sensitivity of AML cells to retinoic acid by the E2F1/autophagy pathway. Cell Prolif 55: e13185, 2022.
23. Cheng Z: The FoxO-Autophagy Axis in Health and Disease. Trends Endocrinol Metab 30: 658-671, 2019.
24. Milan G, Romanello V, Pescatore F, Armani A, Paik JH, Frasson L, Seydel A, Zhao J, Abraham R, Goldberg AL, *et al*: Regulation of autophagy and the ubiquitin-proteasome system by the FoxO transcriptional network during muscle atrophy. Nat Commun 6: 6670, 2015.
25. Lee JW, Nam H, Kim LE, Jeon Y, Min H, Ha S, Lee Y, Kim SY, Lee SJ, Kim EK and Yu SW: TLR4 (toll-like receptor 4) activation suppresses autophagy through inhibition of FOXO3 and impairs phagocytic capacity of microglia. Autophagy 15: 753-770, 2019.
26. Zhang J, Ng S, Wang J, Zhou J, Tan SH, Yang N, Lin Q, Xia D and Shen HM: Histone deacetylase inhibitors induce autophagy through FOXO1-dependent pathways. Autophagy 11: 629-642, 2015.
27. Baek SH and Kim KI: Epigenetic Control of Autophagy: Nuclear Events Gain More Attention. Mol Cell 65: 781-785, 2017.
28. Chen S, Jing Y, Kang X, Yang L, Wang DL, Zhang W, Zhang L, Chen P, Chang JF, Yang XM and Sun FL: Histone H2B monoubiquitination is a critical epigenetic switch for the regulation of autophagy. Nucleic Acids Res 45: 1144-1158, 2017.
29. Artal-Martinez de Narvajas A, Gomez TS, Zhang JS, Mann AO, Taoda Y, Gorman JA, Herreros-Villanueva M, Gress TM, Ellenrieder V, Bujanda L, *et al*: Epigenetic regulation of autophagy by the methyltransferase G9a. Mol Cell Biol 33: 3983-3993, 2013.
30. An PNT, Shimaji K, Tanaka R, Yoshida H, Kimura H, Fukusaki E and Yamaguchi M: Epigenetic regulation of starvation-induced autophagy in Drosophila by histone methyltransferase G9a. Sci Rep 7: 7343, 2017.
31. Wei FZ, Cao Z, Wang X, Wang H, Cai MY, Li T, Hattori N, Wang D, Du Y, Song B, *et al*: Epigenetic regulation of autophagy by the methyltransferase EZH2 through an MTOR-dependent pathway. Autophagy 11: 2309-2322, 2015.
32. Fullgrabe J, Lynch-Day MA, Heldring N, Li W, Struijk RB, Ma Q, Hermanson O, Rosenfeld MG, Klionsky DJ and Joseph B: The histone H4 lysine 16 acetyltransferase hMOF regulates the outcome of autophagy. Nature 500: 468-471, 2013.
33. Hu Z, Gomes I, Horrigan SK, Kravarusic J, Mar B, Arbieva Z, Chyna B, Fulton N, Edassery S, Raza A and Westbrook CA: A novel nuclear protein, 5qNCA (LOC51780) is a candidate for the myeloid leukemia tumor suppressor gene on chromosome 5 band q31. Oncogene 20: 6946-6954, 2001.
34. Mar BG, Bullinger L, Basu E, Schlis K, Silverman LB, Dohner K and Armstrong SA: Sequencing histone-modifying enzymes identifies UTX mutations in acute lymphoblastic leukemia. Leukemia 26: 1881-1883, 2012.
35. MacKinnon RN, Kannourakis G, Wall M and Campbell LJ: A cryptic deletion in 5q31.2 provides further evidence for a minimally deleted region in myelodysplastic syndromes. Cancer Genet 204: 187-194, 2011.
36. Li J, Yu B, Deng P, Cheng Y, Yu Y, Kevork K, Ramadoss S, Ding X, Li X and Wang CY: KDM3 epigenetically controls tumorigenic potentials of human colorectal cancer stem cells through Wnt/β-catenin signalling. Nat Commun 8: 15146, 2017.
37. An MJ, Kim DH, Kim CH, Kim M, Rhee S, Seo SB and Kim JW: Histone demethylase KDM3B regulates the transcriptional network of cell-cycle genes in hepatocarcinoma HepG2 cells. Biochem Biophys Res Commun 508: 576-582, 2019.
38. Sarac H, Morova T, Pires E, McCullagh J, Kaplan A, Cingoz A, Bagci-Onder T, Onder T, Kawamura A and Lack NA: Systematic characterization of chromatin modifying enzymes identifies KDM3B as a critical regulator in castration resistant prostate cancer. Oncogene 39: 2187-2201, 2020.
39. Wang Y, Zhao Y, Wang H, Zhang C, Wang M, Yang Y, Xu X and Hu Z: Histone demethylase KDM3B protects against ferroptosis by upregulating SLC7A11. FEBS Open Bio 10: 637-643, 2020.
40. Kuroki S, Maeda R, Yano M, Kitano S, Miyachi H, Fukuda M, Shinkai Y and Tachibana M: H3K9 Demethylases JMJD1A and JMJD1B Control Prospermatogonia to Spermatogonia Transition in Mouse Germline. Stem Cell Reports 15: 424-438, 2020.
41. Saavedra F, Gurard-Levin ZA, Rojas-Villalobos C, Vassias I, Quatrini R, Almouzni G and Loyola A: JMJD1B, a novel player in histone H3 and H4 processing to ensure genome stability. Epigenetics Chromatin 13: 6, 2020.
42. Xu X, Nagel S, Quentmeier H, Wang Z, Pommerenke C, Dirks WG, Macleod RAF, Drexler HG and Hu Z: KDM3B shows tumor-suppressive activity and transcriptionally regulates HOXA1 through retinoic acid response elements in acute myeloid leukemia. Leuk Lymphoma 59: 204-213, 2018.
43. Xu X, Wang L, Hu L, Dirks WG, Zhao Y, Wei Z, Chen D, Li Z, Wang Z, Han Y, *et al*: Small molecular modulators of JMJD1C preferentially inhibit growth of leukemia cells. Int J Cancer 146: 400-412, 2020.
44. Kim JY, Kim KB, Eom GH, Choe N, Kee HJ, Son HJ, Oh ST, Kim DW, Pak JH, Baek HJ, *et al*: KDM3B is the H3K9 demethylase involved in transcriptional activation of lmo2 in leukemia. Mol Cell Biol 32: 2917-2933, 2012.
45. Li S, Ali S, Duan X, Liu S, Du J, Liu C, Dai H, Zhou M, Zhou L, Yang L, *et al*: JMJD1B demethylates H4R3me2s and H3K9me2 to facilitate gene expression for development of hematopoietic stem and progenitor cells. Cell Rep 23: 389-403, 2018.
46. Goldstein LD, Cao Y, Pau G, Lawrence M, Wu TD, Seshagiri S and Gentleman R: Prediction and Quantification of Splice Events from RNA-Seq Data. PLoS One 11: e0156132, 2016.
47. Love MI, Huber W and Anders S: Moderated estimation of fold change and dispersion for RNA-seq data with DESeq2. Genome Biology 15: 550, 2014.
48. Livak KJ and Schmittgen TD: Analysis of relative gene expression data using real-time quantitative PCR and the 2(-Delta Delta C(T)) method. Methods 25: 402-408, 2001.
49. Hosokawa N, Sasaki T, Iemura S, Natsume T, Hara T and Mizushima N: Atg101, a novel mammalian autophagy protein interacting with Atg13. Autophagy 5: 973-979, 2009.
50. Itakura E, Kishi C, Inoue K and Mizushima N: Beclin 1 forms two distinct phosphatidylinositol 3-kinase complexes with mammalian Atg14 and UVRAG. Mol Biol Cell 19: 5360-5372, 2008.
51. Ryu HY, Kim LE, Jeong H, Yeo BK, Lee JW, Nam H, Ha S, An HK, Park H, Jung S, *et al*: GSK3B induces autophagy by phosphorylating ULK1. Exp Mol Med 53: 369-383, 2021.
52. Matsunaga K, Morita E, Saitoh T, Akira S, Ktistakis NT, Izumi T, Noda T and Yoshimori T: Autophagy requires endoplasmic reticulum targeting of the PI3-kinase complex via Atg14L. J Cell Biol 190: 511-521, 2010.
53. Birgisdottir AB, Mouilleron S, Bhujabal Z, Wirth M, Sjottem E, Evjen G, Zhang W, Lee R, O'Reilly N, Tooze SA, *et al*: Members of the autophagy class III phosphatidylinositol 3-kinase complex I interact with GABARAP and GABARAPL1 via LIR motifs. Autophagy 15: 1333-1355, 2019.
54. Weidberg H, Shvets E, Shpilka T, Shimron F, Shinder V and Elazar Z: LC3 and GATE-16/GABARAP subfamilies are both essential yet act differently in autophagosome biogenesis. EMBO J 29: 1792-1802, 2010.
55. Pankiv S, Alemu EA, Brech A, Bruun JA, Lamark T, Overvatn A, Bjorkoy G and Johansen T: FYCO1 is a Rab7 effector that binds to LC3 and PI3P to mediate microtubule plus end-directed vesicle transport. J Cell Biol 188: 253-269, 2010.
56. Fu MM, Nirschl JJ and Holzbaur ELF: LC3 binding to the scaffolding protein JIP1 regulates processive dynein-driven transport of autophagosomes. Dev Cell 29: 577-590, 2014.
57. Nguyen TN, Padman BS, Usher J, Oorschot V, Ramm G and Lazarou M: Atg8 family LC3/GABARAP proteins are crucial for autophagosome-lysosome fusion but not autophagosome formation during PINK1/Parkin mitophagy and starvation. J Cell Biol 215: 857-874, 2016.
58. Ebner P, Poetsch I, Deszcz L, Hoffmann T, Zuber J and Ikeda F: The IAP family member BRUCE regulates autophagosome-lysosome fusion. Nat Commun 9: 599, 2018.
59. Zhang X, Wang L, Lak B, Li J, Jokitalo E and Wang Y: GRASP55 Senses Glucose Deprivation through O-GlcNAcylation to Promote Autophagosome-Lysosome Fusion. Dev Cell 45: 245-61.e6, 2018.
60. Mansuy-Schlick V, Tolle F, Delage-Mourroux R, Fraichard A, Risold PY and Jouvenot M: Specific distribution of gabarap, gec1/gabarap Like 1, gate16/gabarap Like 2, lc3 messenger RNAs in rat brain areas by quantitative real-time PCR. Brain Res 1073-1074: 83-87, 2006.

61. Tolle F, Risold PY, Mansuy-Schlick V, Rossi E, Boyer-Guittaut M, Fraichard A and Jouvenot M: Specific regional distribution of gec1 mRNAs in adult rat central nervous system. Brain Res 1210: 103-115.
62. Bollaert E, Claus M, Vandewalle V, Lenglez S, Essaghir A, Demoulin JB and Havelange V: MiR-15a-5p confers chemoresistance in acute myeloid leukemia by inhibiting autophagy induced by daunorubicin. Int J Mol Sci 22: 5153, 2021.
63. Wang X, Fan H, Xu C, Jiang G, Wang H and Zhang J: KDM3B suppresses APL progression by restricting chromatin accessibility and facilitating the ATRA-mediated degradation of PML/RARalpha. Cancer Cell Int 19: 256, 2019.
64. Jung H and Seo SB: Histone lysine demethylase 3B (KDM3B) regulates the propagation of autophagy via transcriptional activation of autophagy-related genes. PLoS One 15: e0236403, 2020.
65. Hervouet E, Claude-Taupin A, Gauthier T, Perez V, Fraichard A, Adami P, Despouy G, Monnien F, Algros MP, Jouvenot M, *et al*: The autophagy GABARAPL1 gene is epigenetically regulated in breast cancer models. BMC Cancer 15: 729, 2015.
66. Zhang Y, Wang F, Han L, Wu Y, Li S, Yang X, Wang Y, Ren F, Zhai Y, Wang D, *et al*: GABARAPL1 negatively regulates Wnt/β-catenin signaling by mediating Dvl2 degradation through the autophagy pathway. Cell Physiol Biochem 27: 503-512, 2011.